TABLE I. Summary of shock-wave compression measurements on 30% and 36% Ni–Fe alloys.

u_0[a] (mm/μsec)	Specimen thickness (mm)	Impact Surface u_i[b] (mm/μsec)	Impact Surface σ_i[c] (kbar)	Propagated Profile U_{se}[d] (mm/μsec)	Propagated Profile σ_e[f] (kbar)	Propagated Profile $(V/V_0)_e$[g]	Propagated Profile σ_p[h] (kbar)	Propagated Profile $(V/V_0)_p$[i]	Propagated Profile u_p[i] (mm/μsec)
				30% Ni–70% Fe fcc					
0.2709	12.81	0.1355	...	5.06	4.6	0.9978	45.4	0.9688	0.1313
0.3737	9.538	...	38.5	5.05	4.2	0.9980	40.2	0.9719	0.1167
0.3247	9.538	...	34.4	5.14	4.1	0.9980	34.4	0.9752	0.1018
0.2921	9.525	...	30.0	4.99	3.9	0.9981	29.0	0.9784	0.0872
0.2483	9.525	...	25.8	4.97	2.9	0.9986	25.0	0.9806	0.0749
0.2324	9.525	...	24.0	4.98	3.9	0.9982	23.5	0.9823	0.0702
0.1234	12.81	0.0617	...	5.02–5.00	4.7	0.9977	20.7[k]	0.9847	...
0.0902	12.81	0.0451	...	...	4.4	0.9980	15.9	0.9884	0.0465
0.1380	...	0.0396[l]	14.9[l]	...	...	...	...	0.9914[l]	...
Mean density 8.158 g/cm³; C_0=5.01 mm/μsec[m]; C_s=2.92 mm/μsec[n]; $\bar{\sigma}_e$=4.37 kbar; $\bar{U}_{se}$=5.027 mm/μsec									
				30% Ni–70% Fe bcc					
0.2735	12.79	0.1368	...	5.14	...	...	49.8	0.9708	0.1347
0.1126	12.79	0.0563	...	...	...	...	21.8	0.9876	0.0578
0.0922	12.79	0.0461	...	5.11	...	...	17.9	0.9900	0.0471
Mean density 8.032 g/cm³; C_0=5.23 mm/μsec; $\bar{U}_{se}$=5.13 mm/μsec									
				36% Ni–64% Fe fcc					
0.2853	12.72	0.1427	...	4.91	4.3	0.9977	44.2	0.9646	0.1452
0.1878	12.74	0.0939	...	4.84	5.3	0.9972	30.8	0.9752	0.0968
0.1090	12.74	0.0545	...	...	5.3	0.9972	18.2	0.9865	0.0550
Mean density 8.077 g/cm³; C_0=4.73 mm/μsec; σ_e=5.0 kbar; $\bar{U}_{se}$=4.88 mm/μsec									

[a] Measured impact velocity.
[b] Particle velocity imparted to the specimen for symmetrical impacts.
[c] Stress imparted to the specimen as measured by a quartz gage.
[d] Wave velocity of elastic wave.
[f] Hugoniot elastic limit.
[g] Relative volume at Hugoniot elastic limit.
[h] Maximum stress of plastic wave.
[i] Computed relative volume of plastic wave.
[j] Maximum particle velocity of second plastic wave.
[k] Final stress value was not recorded due to partial experimental failure. The value shown was adjusted to agree with the input value.
[l] Impact surface experiment only. The initial temperature of the sample was 130°C.
[m] Low signal dilatational velocity as obtained by ultrasonic pulsing.
[n] Low signal shear-wave velocity as obtained by ultrasonic pulsing.

used. The velocity of the impacting surface is measured to ±0.5%; therefore, if like materials are used for the projectile and sample, the particle velocity imparted to the sample is known. Also, impacting with a quartz gage enables a measurement of the stress and particle velocity imparted to the sample at the impact face.[14,15] These data provide independent measurements of the shock-wave behavior from that obtained at the conventional measuring station at the back side of the specimen. The redundancy achieved allows cross comparisons of data from a single experiment and greatly increases the confidence in the results since it serves as a quantitative measure of errors in the entire data recording and data reduction process as well as a verification of the assumptions made in reducing the data.

Shock-wave velocity data are needed to compute the stress amplitude in the sample from the observed quartz gauge record of the interface stress. These measurements are accomplished by the arrival times indicated by the impacting and back surface quartz gauges with accurately known time delays interposed between trigger signals for two-gauge records. For the experiments in which an impacting gauge is not used, the discharge of charged coaxial pins is used to indicate impact time. The shock-wave velocity accuracy is ±1%. The absolute error in stress is ±3% with ±1% relative errors. The error in volume change is estimated to be ±2%.

The 30% Ni–70% Fe alloy material was the commercially obtained "Temperature Compensator 30" alloy.[16] The 36% Ni–Fe alloy used was "Invar 36" obtained from the same supplier. After machining to the desired dimensions, the samples were heat treated according to the following schedule. The fcc phase 30% Ni alloy samples were held 2 h at 650°C, then furnace-cooled to 100°C. The bcc phase 30% Ni alloy samples were annealed 2 h at 650°C, furnace cooled to room temperature, then kept in liquid nitrogen for 168 h. The 36% Ni–Fe alloy samples were held 16 h at 900°C, then furnace cooled to 100°C. All elevated temperature treatments were performed in a vacuum of 10^{-6} Torr.

[14] W. J. Halpin, O. E. Jones, and R. A. Graham, ASTM Special Technical Publication No. 336, ASTM (1962).
[15] W. J. Halpin and R. A. Graham, Fourth Symposium on Detonation, U.S. Naval Ordnance Laboratory (October 1965).
[16] The alloys were obtained from the Carpenter Steel Company.

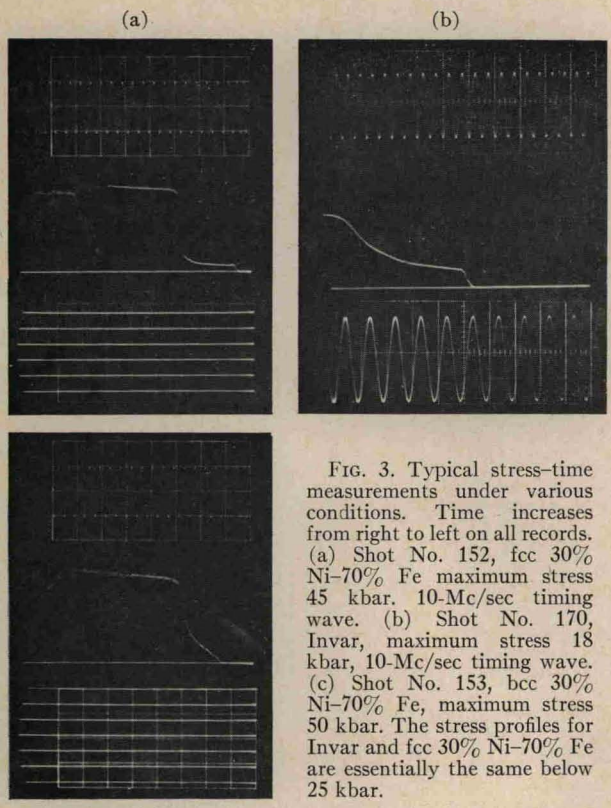

FIG. 3. Typical stress–time measurements under various conditions. Time increases from right to left on all records. (a) Shot No. 152, fcc 30% Ni–70% Fe maximum stress 45 kbar. 10-Mc/sec timing wave. (b) Shot No. 170, Invar, maximum stress 18 kbar, 10-Mc/sec timing wave. (c) Shot No. 153, bcc 30% Ni–70% Fe, maximum stress 50 kbar. The stress profiles for Invar and fcc 30% Ni–70% Fe are essentially the same below 25 kbar.

X-ray examination of the heat-treated samples showed that to the limit of detectability (5%) no minority phase was present. To determine atmospheric pressure elastic constants, typical samples were pulsed ultrasonically with results as shown in Table I. Chemical analyses were obtained on the samples which, for a given alloy, were all cut from the same bar of material. The mean value for the nickel content was 29.53% with a variance of 0.24%.

Since it was desired to measure the change in Curie temperature with pressure, it was necessary to measure the atmospheric-pressure Curie temperature for the 30% Ni–Fe alloy. This was determined by dilatometer measurements on bulk samples and x-ray lattice spacing vs temperature measurements. The value obtained for the Curie temperature from the thermal expansion measurements was 155°±3°C.

RESULTS

Typical stress–time profiles for various materials and various stress regions are shown in Fig. 3. The leading part of the profile results from the transition from elastic to plastic deformation. The sharp rise in stress for the second wave in Fig. 3(a) and the faster arrival time compared with that in Fig. 3(b) is that expected if the input stress is above the transition. Whereas, the slower rise in Fig. 3(b) is that expected if the stress input to the sample is below the transition. The profile in Fig. 3(c) for the bcc alloy was obtained for an imput particle velocity approximately equal to that in Fig. 3(a) for the fcc alloy. The bcc alloy shows a poorly defined precursor region, but, in any event, much faster arrival times are observed for all stress amplitudes as is indicative of lower compressibility.

The excellent time-resolution of the quartz gauge has revealed that few materials give idealized step function stress–time profiles. Hence, to reduce the stress–time profiles to stress–volume points the profile observed must be approximated by a series of small incremental steps constructed around the observed profile. This procedure has the further advantage that corrections can be made for the slightly variable response of the gauge. The solution for the incident stress from the measured interface stress was accomplished for each small increment of stress using the linear mismatch relations and the appropriate shock velocity for each step. The resulting final values can be checked against the measured input conditions to the sample as an over-all check of experimental errors and errors in data reduction. The data obtained on all experiments are tabulated in Table I. Most of the experiments were performed on fcc 30% Ni with less extensive experiments on 36% Ni and bcc 30% Ni.

The resulting stress–volume relations for the 30% Ni alloys are shown in Fig. 4. The cusp in the fcc curve at 4.3 kbar is the mean value observed for the Hugoniot

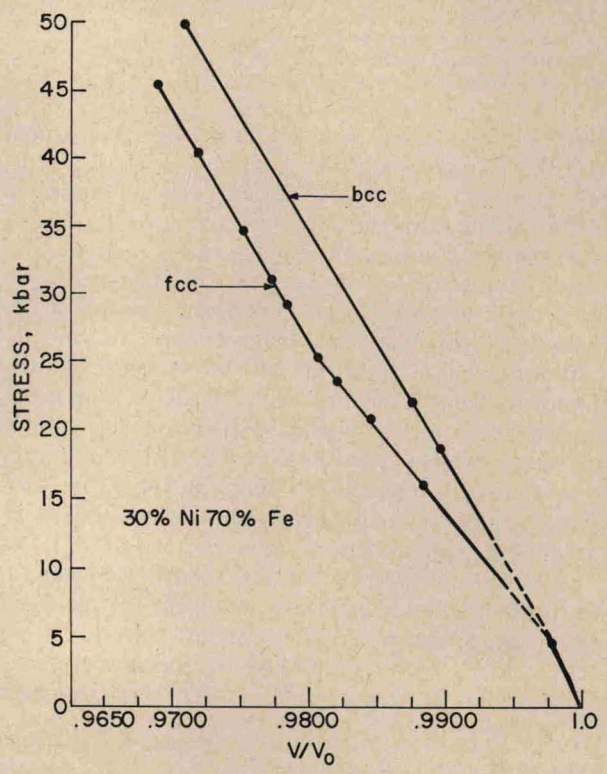

FIG. 4. Stress–volume relation for 30% Ni–70% Fe in the fcc and bcc phases.